Journal of Experimental Pharmacology

Dovepress
Taylor & Francis Group

Open Access Full Text Article

ORIGINAL RESEARCH

High-Concentration Cyanidin-3-O-Glucoside Attenuates Palmitic Acid-Induced Oxidative Stress via ROS Suppression in Pancreatic β-Cells

Sasirin Chitwattananont[1], Sutthipong Sawasvirojwong[2], Chatchai Muanprasat[1,2]

[1]Translational Medicine Graduate Program, Faculty of Medicine Ramathibodi Hospital, Mahidol University, Bangkok, Thailand; [2]Chakri Naruebodindra Medical Institute, Faculty of Medicine Ramathibodi Hospital, Mahidol University, Samutprakarn, Thailand

Correspondence: Chatchai Muanprasat, Chakri Naruebodindra Medical Institute, Faculty of Medicine Ramathibodi Hospital, Mahidol University, Samutprakarn, Thailand, Email chatchai.mua@mahidol.ac.th

Background: Type 2 diabetes mellitus (T2DM) is characterized by progressive β-cell dysfunction driven in part by palmitic acid (PA)-induced lipotoxicity. Cyanidin-3-O-glucoside (C3G) possesses antioxidant properties, but its temporal and mechanistic effects at higher concentrations remain poorly defined.

Objective: This study aimed to investigate the continuous effects of high-concentration of C3G on PA-induced β-cell apoptosis, with emphasis on time-dependent efficacy and underlying antioxidant mechanisms.

Methods: MIN6 cells were treated with PA (500 μM) in the presence or absence of C3G (500 μM). Cell viability was assessed by MTT assay, apoptosis by flow cytometry and cell death assay, oxidative stress by DCFDA and DPPH assays, and ER-stress related C/EBP homologous protein (CHOP) and apoptotic cleaved caspase-3 expression by Western blot analysis.

Results: PA (500 μM) significantly reduced MIN6 cell viability, whereas continuous exposure to C3G (500 μM) restored viability, corresponding to a 40.9% increase ($p < 0.001$) compared with PA treatment alone. Flow cytometry showed that PA reduced live cells from 78.6% to 41.0% and increased early and late apoptotic populations to 27.7% and 28.2%, respectively, whereas C3G co-treatment reduced apoptosis to 17.7%. Consistently, cell death assays confirmed that C3G lowered apoptotic cells from 30.7% to 5.0% ($p < 0.001$ vs PA-treated groups) and restored viability to 93.1%, comparable to vehicle controls. Reactive oxygen species (ROS) assays, including DCFDA and DPPH, further demonstrated that C3G reduced PA-induced ROS by 26.5% ($p < 0.01$ vs PA alone), consistent with free radical-scavenging activity. Western blot analyses revealed that PA markedly upregulated CHOP and cleaved caspase-3, which was suppressed by co-treatment with C3G, confirming the attenuation by C3G of ER stress-mediated apoptotic signaling. These findings imply that C3G rapidly counteracts oxidative stress-induced apoptosis.

Conclusion: High-concentration C3G mitigates PA-induced oxidative stress and ER stress-associated apoptosis in β-cells, supporting its potential as a therapeutic agent for T2DM.

Plain Language Summary: Type 2 diabetes mellitus (T2DM) is a common metabolic disorder driven by progressive β-cell dysfunction, in which elevated free fatty acids, particularly palmitic acid (PA), induce oxidative stress-mediated apoptosis that accelerates disease progression. Cyanidin-3-O-glucoside (C3G) has been identified as a promising agent for protecting β-cells through its antioxidant capacity. This study aimed to investigate the protective role of high-concentration C3G against PA-induced β-cell apoptosis, focusing particularly on its efficacy in a dose- and time-dependent manner as well as the underlying antioxidant mechanism. We found that high concentrations of C3G mitigate PA-induced β-cell apoptosis by fully neutralizing reactive oxygen species (ROS) accumulation and downregulating ER stress-related apoptotic pathways. Altogether, our findings emphasized that high-concentration of C3G exerted a rapid and potent protective effect against oxidative stress-induced apoptosis, thereby highlighting its translational potential in the treatment of T2DM patients.

Keywords: diabetes, oxidative stress, β-cells, palmitic acid, cyanidin-3-O-glucoside

https://doi.org/10.2147/JEP.S562755
Received: 23 August 2025
Accepted: 19 March 2026
Published: 23 May 2026

Introduction

Type 2 diabetes mellitus (T2DM) is one of the most prevalent non-communicable diseases (NCDs) worldwide.[1,2] It arises from multifactorial factors, including genetic predisposition and environmental influences. Over the past few decades, the global incidence of T2DM has increased two- to threefold, with a notable surge among individuals under the age of 40.[3] The rise in obesity is a key contributing factor, driving insulin resistance (IR) and β-cell dysfunction.[4] Such pathologic mechanisms contribute to persistent hyperglycemia and reinforce the vicious cycle of disease progression. To date, accumulating evidence indicates a strong association between excessive adiposity and the pathogenesis of T2DM, primarily mediated by chronic low-grade systemic inflammation driven by elevated levels of circulating saturated free fatty acids (FFAs), particularly palmitic acid (PA).[5]

PA (C16:0), a long-chain saturated fatty acid, is a predominant lipid implicated in metabolic disturbances underlying T2DM.[6,7] PA activates key pro-inflammatory signaling pathways, including c-Jun N-terminal kinase (JNK) and inhibitory kappa B kinase beta (IKKβ), leading to serine phosphorylation of insulin receptor substrate-1 (IRS-1) and consequent impairment of insulin receptor function.[8–11] Furthermore, elevated PA levels and hyperglycemia synergistically induce unfolded protein response (UPR)-mediated apoptosis by triggering endoplasmic reticulum (ER) stress, thereby exacerbating β-cell dysfunction.[12,13] Chronic exposure to high concentrations of PA also aggravates lipotoxicity and induces β-cell apoptosis through oxidative stress, mediated by increased reactive oxygen species (ROS) production, as demonstrated in both in vitro and in vivo models.[14–16]

Cyanidin 3-O-glucoside (C3G) (Figure 1), a natural anthocyanin abundant in pigmented fruits and grains such as berries and black rice, has attracted considerable attention for its potent anti-inflammatory and antioxidant properties.[17,18] C3G has been shown to activate AMP-activated protein kinase (AMPK), thereby reducing inflammation in metabolic tissues, including muscle, liver, and adipose tissue.[19–22] In pancreatic β-cells, low doses of C3G mitigate PA-induced lipotoxicity by attenuating ER stress and oxidative damage, likely via upregulation of antioxidant enzymes such as superoxide dismutase (SOD) and catalase (CAT).[23–25] In db/db diabetic mice, C3G improves islet morphology and glycemic control, underscoring its potential in preserving β-cell function and preventing apoptosis.[26] By contrast, other antioxidant agents, including N-acetylcysteine (NAC) and Trolox, which were widely used as experimental positive controls in several studies, had been reported to attenuate PA-induced oxidative stress and β-cell apoptosis; however, their protective effects are often transient, dose-dependent, and limited by poor bioavailability or incomplete mechanistic characterization, resulting in uncertain translational applicability.[27,28] Indeed, NAC lowered basal insulin release and

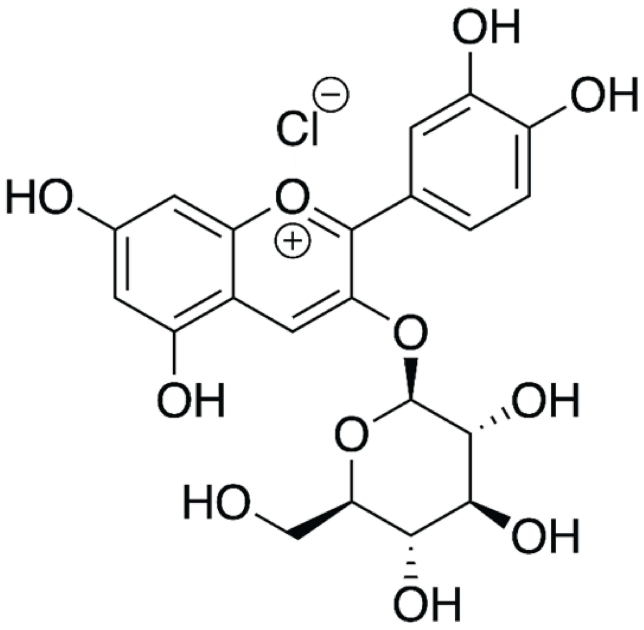

Figure 1 Chemical structure of Cyanidin 3-O-glucoside (C3G).

improved glucose-stimulated insulin secretion (GSIS) under physiological glucose, but failed to sustain benefit under prolonged lipotoxicity.[29] Furthermore, Trolox demonstrated concentration-dependent dual activity, acting as an antioxidant at low doses but a pro-oxidant at higher levels, with short-term efficacy only and lacking of clinical relevance.[30] Overall, recovery of β-cell viability with these agents was typically modest (~30–50%), reflecting their restricted translational potential. In contrast, C3G, a naturally occurring dietary anthocyanin with demonstrated metabolic benefits in human supplementation studies, offers greater translational plausibility for β-cell preservation strategies.[31] Although low-dose C3G achieved comparable recovery (~40–50%) with added mechanistic benefits such as AMPK activation and endogenous enzyme upregulation,[23–26] the protective efficacy of high-dose C3G during continuous PA exposure on β-cell viability, as well as its temporal and mechanistic actions, had not been elucidated. Therefore, this study aimed to investigate the protective effects of high-concentration C3G on PA-induced β-cell dysfunction in MIN6 cells, with a focus on temporal efficacy and underlying antioxidant mechanisms.

Materials and Methods

Materials

Dulbecco's Modified Eagle's Medium (DMEM)-high glucose (HG), fetal bovine serum (FBS), trypsin-EDTA, streptomycin, penicillin, ethidium homodimer-1 (EthD-1), and Hoechst 33342 were purchased from Thermo Fisher Scientific Inc (Waltham, MA, USA). PA was received from Sigma-Aldrich Co (St. Louis, MO, USA). C3G (>97% purity) was purchased from Biolink (Sandnes, Norway) and dissolved in dimethyl sulfoxide (DMSO; <0.1% final concentration). BD Pharmingen™ FITC Annexin V Apoptosis Detection Kit I was obtained from BD Biosciences (Franklin Lakes, NJ, USA). Primary antibodies against C/EBP homologous protein (CHOP; mouse), cleaved caspase-3 (rabbit), and β-actin (rabbit), as well as horse anti-mouse and goat anti-rabbit horseradish peroxidase (HRP)-linked secondary antibodies, were obtained from Cell Signaling Technology (Beverly, MA, USA). Skim milk and Clarity™ Western ECL substrate were purchased from Bio-rad (Hercules, CA, USA). Six-well plates were purchased from Corning Life Sciences (Corning, NY, USA).

PA Preparation

PA was prepared as a sodium palmitate-bovine serum albumin (BSA) conjugate following established protocols.[32] To generate the conjugate, sodium palmitate was dissolved in distilled water and maintained at 70°C for approximately 30 min, or until the solution became completely transparent. In parallel, BSA was dissolved at 10% (w/v) in distilled water and incubated at 55°C for 30 min. The hot sodium palmitate solution was then added slowly to the warmed BSA solution. The resulting PA-BSA complex stock contained 10 mM PA with ~1.5 mM BSA, corresponding to a ~6:1 molar ratio of PA:BSA. For experimental treatments, the PA-BSA stock was diluted in serum-free DMEM-HG to the desired final concentrations. In the vehicle group, the cells were treated with the equivalent concentration of BSA.

Cell Culture

MIN6 cells were purchased from American Type Culture Collection (ATCC; Manassas, VA, USA). Ethics approval was not required as the study used established cell lines and did not involve human participants or live animals. Cells were cultured in Dulbecco's Modified Eagle's Medium, High Glucose (DMEM-HG), supplemented with 10% (v/v) fetal bovine serum (FBS) and 1% (v/v) penicillin-streptomycin. The cells were maintained in a humidified incubator at 37°C in an atmosphere of 95% air and 5% CO_2. Cells at passages 17 to 23 were used for experiments once they reached 80–90% confluence and were subsequently trypsinized for subculture.

Cell Viability Assay

MIN6 cell viability was evaluated using the 3-(4,5-Dimethyl-2-thiazolyl)-2,5-diphenyl-2H-tetrazolium Bromide (MTT) assay. MTT was purchased from Sigma-Aldrich Co. (St. Louis, MO, USA). In brief, cells were seeded in 96-well plates at a density of 1×10^5 cells/well and cultured until reaching approximately 70% confluence. The cells were then treated with serum-free medium containing BSA (75 μM) and DMSO (final concentration <0.1%) as vehicle, PA (500 μM), or

PA combined with various concentrations of C3G (10, 20, 50, 100, 200, and 500 μM) for 24 hours. After treatment, the medium was replaced with MTT working solution (stock 5 mg/mL) diluted to a final concentration of 0.5 mg/mL in serum-free DMEM-HG. Cells were incubated for 4 hours at 37°C in the dark to allow viable cells to reduce MTT to formazan. The solution was then removed, and 100 μL of DMSO was added to each well to dissolve the formazan crystals and terminate the reaction. Cell viability was determined by measuring absorbance at 573 nm using a spectrophotometer.

Flow Cytometry

A total of 1×10^6 MIN6 cells per well were plated in 6-well plates and cultured until 70% confluence was achieved. Cells were then treated with vehicle (BSA and DMSO), PA (500 μM), C3G (500 μM) or PA combined with C3G for 24 hours. After treatment, cells were harvested, washed with cold PBS, and resuspended in Annexin V binding buffer. Annexin V-FITC (5 μL) and PI (5 μL) were added to the cell suspension and incubated for 5 minutes at room temperature in the dark. Apoptotic cells were analyzed using a flow cytometer (BD Accuri™ C6 Plus Flow Cytometer). Cells stained with Annexin V-FITC alone (Annexin V^+/PI^-) were classified as early apoptotic, while cells stained with both Annexin V-FITC and PI (Annexin V^+/PI^+) were considered late apoptotic. Cells detected as Annexin V-/PI- were labeled as normal live cells, while cells highlighted with PI alone (Annexin V-/PI+) were indicated as dead cells.

Cell Death Assay

MIN6 cells were plated in black 96-well plates at a density of 1×10^5 cells per well and cultured until reaching approximately 70% confluence. The cells were then exposed to PA (500 μM) or PA combined with cyanidin-3-O-glucoside (500 μM) for 24 hours, followed by co-staining with Hoechst 33342 (10 μg/mL) and Ethidium homodimer-1 (EthD-1, 2 μM) for 10 minutes. Cells labeled only with Hoechst 33342 were classified as viable. Early apoptotic cells exhibited nuclear condensation with intact plasma membranes, resulting in increased Hoechst fluorescence. Late apoptotic cells were identified by dual staining with Hoechst 33342 and EthD-1, whereas necrotic cells were detected by only EthD-1 staining.

DCFDA Assay

To quantify intracellular ROS levels, the dichlorofluorescin diacetate (DCFDA) assay was performed as described previously.[33] Briefly, MIN6 cells were seeded at a density of 1×10^5 cells per well in 96-well plates and cultured for 24 hours. Cells were then treated with PA (500 μM), with or without C3G (500 μM), for an additional 24 hours. Following treatment, cells were incubated with 25 μM DCFDA at 37°C for 45 minutes. After incubation, cells were washed once with phosphate-buffered saline (PBS) and stained with Hoechst 33342 (1:1000) for 5 minutes at 37°C. Fluorescence intensity was measured using a BioTek Synergy Neo2 Hybrid Multi-Mode Reader, and representative images were captured using a confocal fluorescence microscope.

DPPH Assay

The antioxidant activity of C3G was evaluated using the 2,2-diphenyl-1-picrylhydrazyl (DPPH) radical scavenging assay. DPPH was obtained from Sigma-Aldrich Co. (St. Louis, Missouri, USA). In short, a 0.2 mM DPPH solution was prepared in ethanol and protected from light to maintain stability. Various concentrations of C3G, along with Trolox (used as a positive control), were mixed with an equal volume of DPPH solution in a 96-well microplate. The reaction mixtures were incubated at room temperature (25°C) in the dark for 30 minutes to prevent photodegradation. After incubation, the absorbance was measured at 517 nm using a Synergy™ Neo2 Multi-Mode Microplate Reader (BioTek Instruments, Winooski, VT, USA) for calculation of radical scavenging activity.

Western Blot Analysis

MIN6 cells were seeded in 6-well plates at 1×10^6 cells per well and cultured to ~70% confluence before exposure to 500 μM PA, with or without 500 μM C3G, for 24 hours. After treatment, cells were lysed in RIPA buffer, and protein extracts were obtained by centrifugation at 12,000 rpm for 30 minutes at 4°C. Equal amounts of protein were separated

on 10% SDS-PAGE gels at 80 V and transferred to nitrocellulose membranes at 220 mA. Membranes were blocked with 10% skim milk for 1 hour, then incubated overnight at 4°C with primary antibodies against cleaved caspase-3, CHOP, and β-actin (1:500). Following TBST washes, membranes were incubated for 1 hour at room temperature with HRP-conjugated goat anti-rabbit IgG. Protein bands were visualized using Clarity™ Western ECL substrate and quantified with ImageJ software (National Institutes of Health, Bethesda, MD, USA).

Statistics

Data were presented as means ± standard error of the mean (S.E.M.). Statistical comparisons between groups were performed using one-way analysis of variance (ANOVA), followed by Tukey's post hoc test. All statistical analyses were conducted using GraphPad Prism software (GraphPad Software, San Diego, CA, USA). A p-value of <0.05 was considered statistically significant.

Results

Effect of PA on the Viability of MIN6 Pancreatic β-Cells

Since elevated serum free fatty acids, particularly PA, have been associated with insulin resistance,[34] we first investigated the effect of PA on β-cell viability using the MIN6 cell line in vitro. Cells were treated with various concentrations of PA (50, 100, 500, and 1000 μM) in a dose-dependent manner for 24 hours. Subsequently, cell viability was assessed using the MTT assay. The results showed that PA treatment resulted in a dose-dependent decrease in β-cell viability, with approximately a 56.4% reduction at 50 μM (56.4 ± 5.9, ***$p < 0.001$) and the greatest cytotoxic effect observed at 500 μM (37.0 ± 5.9, ***$p < 0.001$) (Figure 2). Notably, PA concentrations between 50 and 150 μM are considered to approximate the physiological range of circulating free fatty acids in humans,[7] whereas higher concentrations (≥500 μM) reflect pathological conditions and produced a plateau effect, with maximal cytotoxicity reached at 500 μM and no further significant increase at 1000 μM. These results support the role of PA as a lipotoxic compound that impairs pancreatic β-cell viability in a concentration-dependent manner.

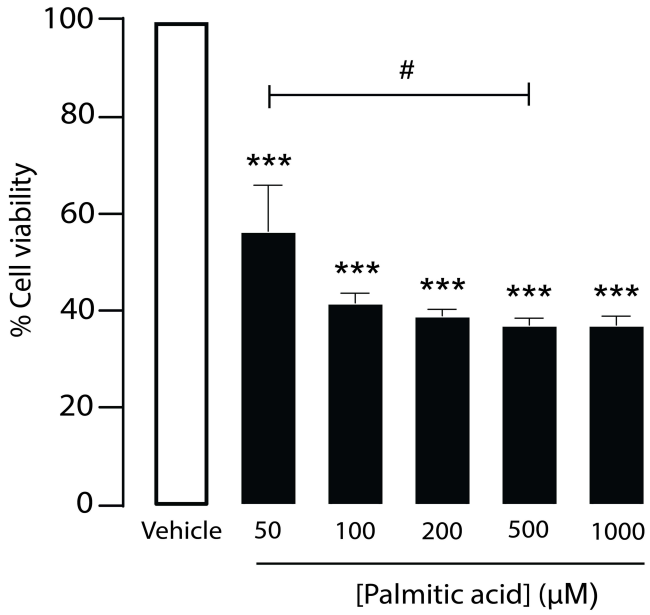

Figure 2 Effect of palmitic acid (PA) on β-cell viability. Dose-dependent effect of PA on MIN6 cell viability. Cell viability was assessed by MTT assay and quantified by measuring absorbance at 573 nm. Data were presented as means ± S.E.M. (n = 6, representing six independent cell preparations; each condition measured in duplicate). ***$p < 0.001$, PA-treated groups compared with the vehicle group; #$p < 0.05$, PA (50 μM) group compared with the PA (500 μM) group.

https://doi.org/10.2147/JEP.S562755

Effect of C3G Against PA on the Viability of MIN6 Pancreatic β-Cells

C3G is well-known for its antioxidant activity.[20] To determine whether C3G can counteract the reduction in β-cell viability induced by PA, MIN6 cells were treated for 24 hours with either 500 μM PA alone or co-treated with 500 μM PA and increasing concentrations of C3G (10, 20, 50, 100, 200, and 500 μM) (Figure 3A). As shown in Figure 3B, 500 μM PA significantly reduced β-cell viability (37.6 ± 4.6 of 500 μM PA vs vehicle, ***p < 0.001) whereas C3G

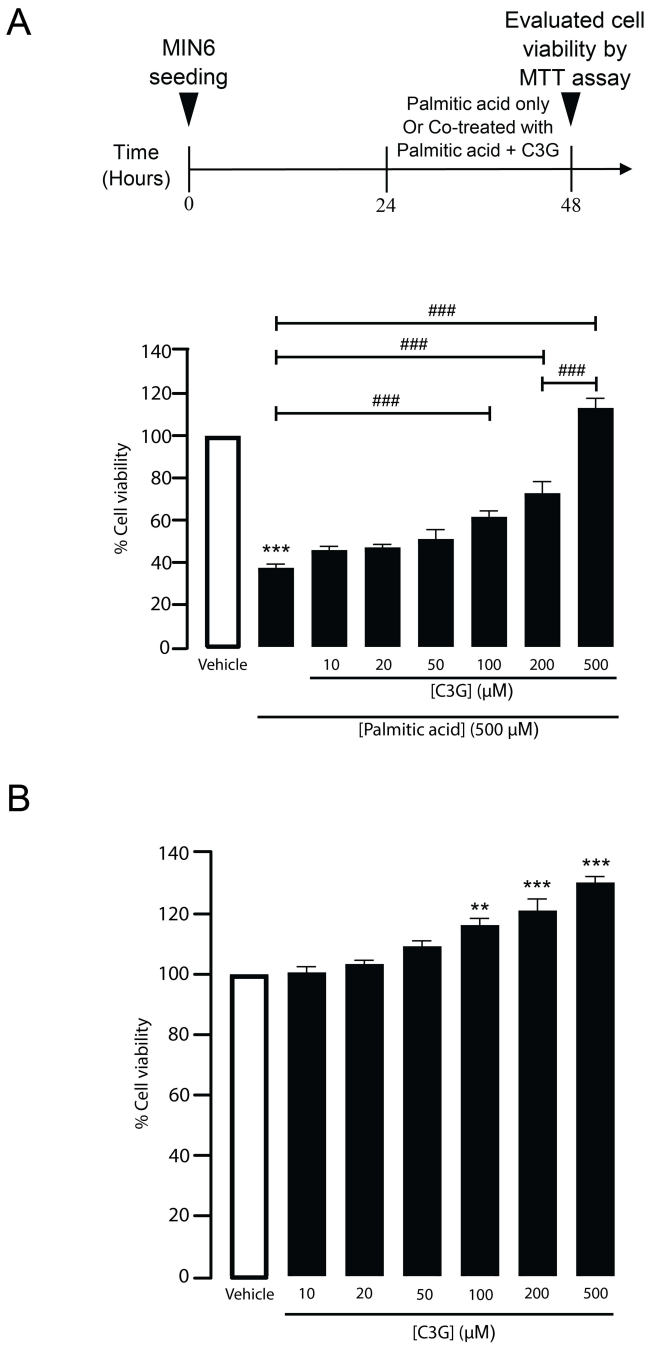

Figure 3 Cyanidin 3-O-glucoside (C3G) enhances MIN6 cell viability under palmitic acid (PA)-induced stress. (**A**) Schematic illustration of the protocol: MIN6 cells were co-treated with 500 μM PA and varying concentrations of C3G (10, 20, 50, 100, 200, or 500 μM) for 24 hours. Cell viability was assessed by measuring absorbance at 573 nm. ***p < 0.001, PA-treated group compared to the vehicle group; ###p < 0.001 vs PA alone (for C3G 100, 200, and 500 μM) and vs C3G 200 μM group (for C3G 500 μM). Data are presented as mean ± S.E.M. (n = 6, representing six independent cell preparations; each condition measured in duplicate). (**B**) Dose-dependent effect of C3G on MIN6 cell viability. MIN6 cells were treated with increasing concentrations of C3G for 24 hours. Cell viability was measured using absorbance at 573 nm. **p < 0.01; ***p < 0.001, compared to the vehicle group. Data are presented as mean ± S.E.M. (n = 3, representing three independent cell preparations; each condition measured in duplicate).

https://doi.org/10.2147/JEP.S562755

enhanced β-cell viability in a concentration-dependent manner, with 500 μM C3G fully restoring viability compared with PA alone (113.3 ± 4.6 of 500 μM PA vs 500 μM PA + 500 μM C3G, $^{###}p < 0.001$). In addition, C3G alone, at concentrations ranging from 10 to 500 μM, did not reduce β-cell viability after 24 hours of treatment (Figure 3B). These findings indicate that C3G effectively mitigates PA-induced cytotoxicity in pancreatic β-cells in a dose-dependent manner.

Role of High-Concentration C3G as a Cytoprotective Compound Against PA-Induced β-Cell Apoptosis

To evaluate whether high concentrations of C3G can protect against PA-induced cytotoxicity, MIN6 cells were co-treated with 500 μM PA and 500 μM C3G for 24 hours and analyzed by flow cytometry using Annexin V/PI staining. As a reference, PA treatment alone significantly decreased β-cell viability by reducing the proportion of live cells from 78.6% to 41.0%, while increasing early apoptotic cells from 17.9% to 27.7% and late apoptotic cells from 3.3% to 28.2% (Figure 4A–C). These findings indicate that the reduction in β-cell viability upon PA exposure is attributable to apoptosis. Interestingly, co-treatment with C3G at high concentration markedly reduced the proportion of PA-induced dying cells, including both early and late stages of apoptosis, from 59.4% to 17.7%. In contrast, treatment with C3G alone had no significant effect, as the proportions of viable and apoptotic cells remained ~80% and ~20%, respectively. Necrotic cells remained minor across all groups (~0.1–1.6%), and the exposure to C3G alone did not increase necrosis. In accordance with the flow cytometry findings, a cell death assay was conducted to validate the protective effect of high concentrations of C3G against PA-induced cytotoxicity. MIN6 cells were co-treated with PA (500 μM) and C3G (500 μM) for 24 hours, and viable and apoptotic cells were quantified by EthD-1/Hoechst co-staining. PA exposure reduced β-cell viability from 86.0% to 67.7%, with early apoptotic cells increasing from 5.0 to 9.0% and late apoptotic cells from 7.3% to 21.6%. Co-treatment with C3G significantly attenuated apoptosis, lowering the combined apoptotic population from 30.7% to 5.0%, while restoring viable cells to 93.1%, comparable to vehicle levels (Figure 5A and B). Collectively, these results demonstrate that C3G attenuates PA-induced β-cell apoptosis without exerting cytotoxic effects on its own.

Continuous Presence of High-Concentration C3G is Required to Protect β-Cells from PA-Induced Cytotoxicity

To clarify the mechanism by which C3G mitigates PA-induced cytotoxicity, we aimed to determine if its protective effect results from pretreatment alone or necessitates its presence during PA exposure. MIN6 cells were divided into two experimental groups for cell viability assays: cells pretreated with C3G (500 μM) for 24 hours followed by PA (500 μM) alone and cells pretreated with C3G and then co-treated with PA and C3G for an additional 24 hours. Interestingly, C3G pretreatment without continued exposure failed to confer protection (Figure 6A), whereas co-treatment with PA and C3G significantly improved β-cell viability at all concentrations (Figure 6B). These findings indicate that the protective effect of high-dose C3G against PA-induced cytotoxicity depends on its continued presence during the lipotoxic challenge, suggesting that C3G may exert an acute protective effect against PA-induced cytotoxicity.

Assessment of the Antioxidant Effect of High-Concentration C3G Against PA-Induced Intracellular ROS Elevation

ROS play a pivotal role in inducing cell apoptosis. Previous studies have demonstrated that PA treatment increases ROS production in β-cells, contributing to oxidative stress and ultimately leading to cell death.[35,36] To investigate whether high concentrations of C3G can counteract PA-induced ROS generation, MIN6 cells were treated with PA (500 μM) alone or co-treated with PA (500 μM) and C3G (500 μM) for 24 hours. Intracellular ROS levels were then assessed using the DCFDA assay. As shown in Figure 7A and B, PA increased intracellular ROS to 128.7 ± 7.4, $p < 0.01$, whereas co-treatment with C3G reduced ROS to 102.2 ± 7.4, $p < 0.01$. These results suggested that C3G exhibits antioxidant activity by reducing intracellular ROS levels, thereby protecting β-cells from PA-induced oxidative stress.

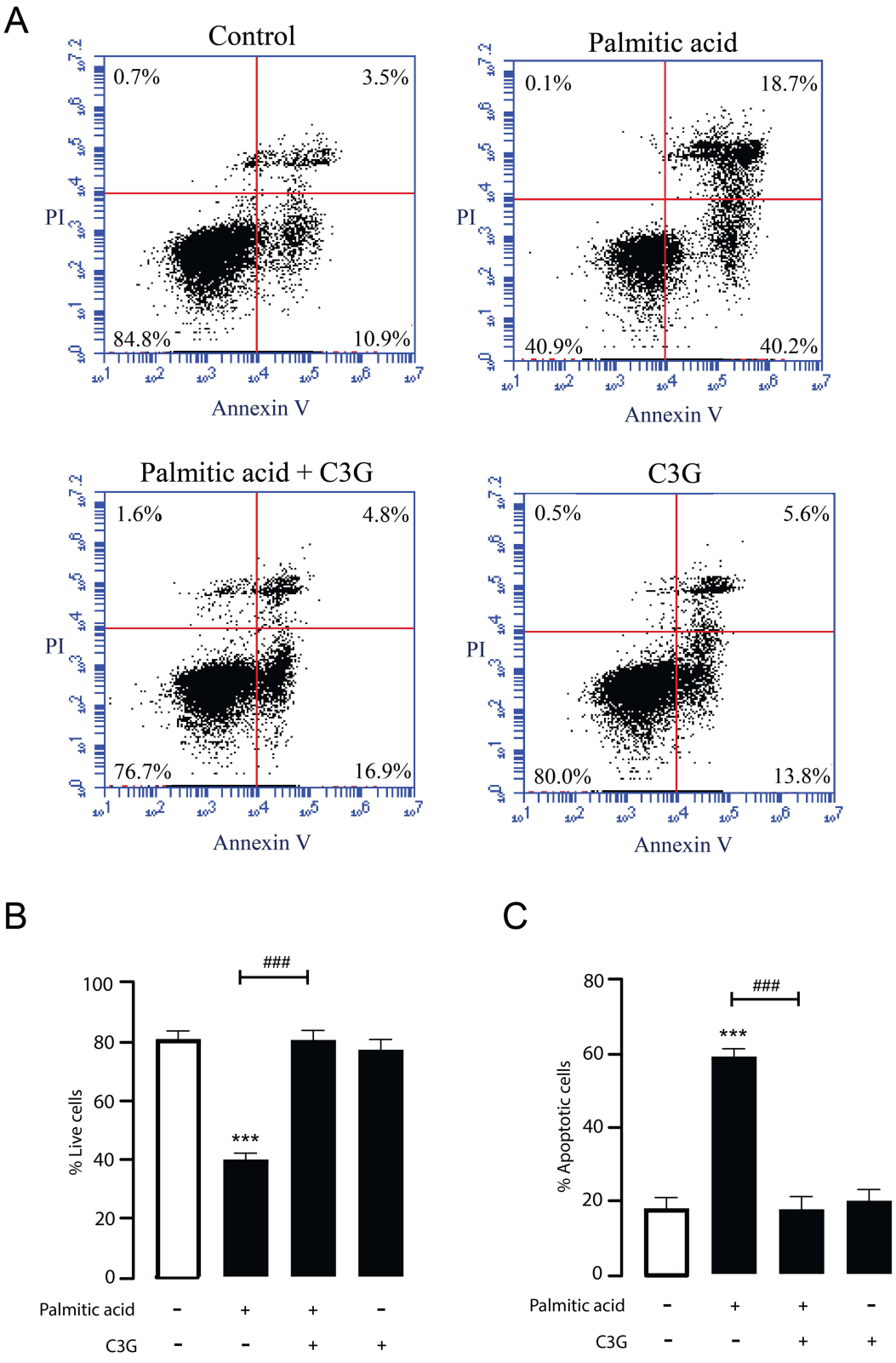

Figure 4 Protective effect of Cyanidin 3-O-glucoside (C3G) against palmitic acid (PA)-induced apoptosis in MIN6 cells. (**A**) Representative flow cytometry plots illustrate the effects of 500 μM C3G on MIN6 cell survival under 500 μM PA treatment. The lower left quadrant (Annexin V–/PI–) indicates viable cells, while the upper left quadrant (Annexin V–/PI+) represents necrotic cells. Early apoptotic cells are shown in the lower right quadrant (Annexin V+/PI–), and late apoptotic cells in the upper right quadrant (Annexin V+/PI+). Data are representative of four independent experiments. (**B** and **C**) Quantitative analysis of flow cytometry data for assessing the percentage of viable and apoptotic cells. Bar graphs show the distribution of live (Annexin V–/PI–) and apoptotic (Annexin V+/PI+ and Annexin V+/PI–) cell populations under each treatment condition. ***$p < 0.001$ vs vehicle; ###$p < 0.001$ vs PA (500 μM) alone. Data are presented as mean ± S.E.M. (n = 4, representing four independent cell preparations).

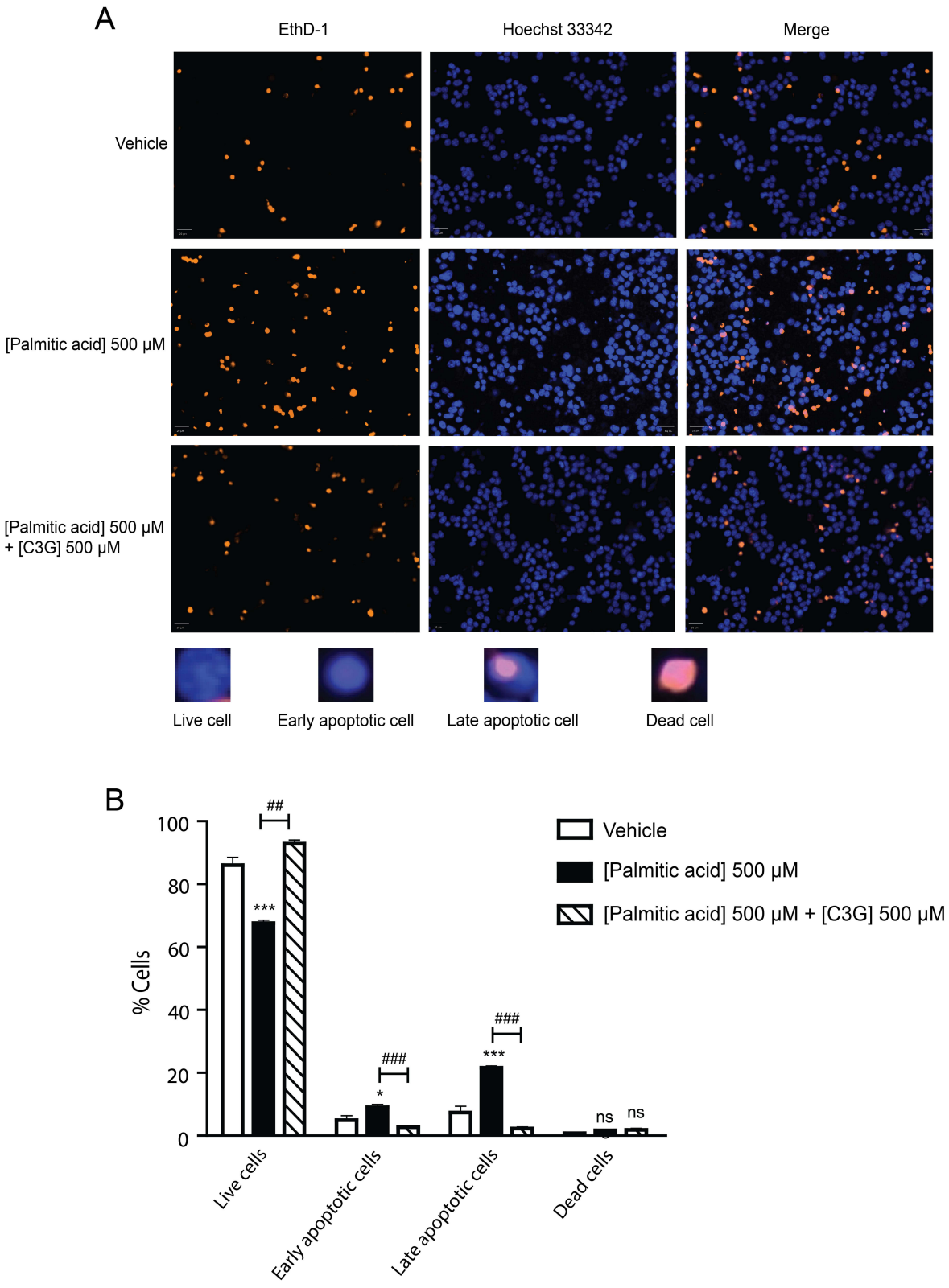

Figure 5 Validation of the Cyanidin 3-O-glucoside (C3G) protection against palmitic acid (PA)-induced apoptosis in MIN6 cells. (**A**) Cell death assay immunofluorescence staining of Hoechst 33342 (blue) and EthD-1 (Orange) of MIN6 cells after 24 h treatment. Representative images illustrate viable, early apoptotic, late apoptotic, and dead cells. (**B**) Quantitative evaluation of Hoechst/EthD-1 co-staining was used to determine the percentage of live and apoptotic MIN6 cells in each treatment condition. Data are expressed as mean ± S.E.M. (n = 4, representing four independent cell preparations; each condition measured in duplicate). * $p < 0.05$; *** $p < 0.001$ compared to vehicle, $^{\#\#}p < 0.01$; $^{\#\#\#}p < 0.001$, PA-treated groups (500 μM) compared to PA + C3G groups (500 μM), ns, no significant difference vs vehicle or PA + C3G group.

https://doi.org/10.2147/JEP.S562755

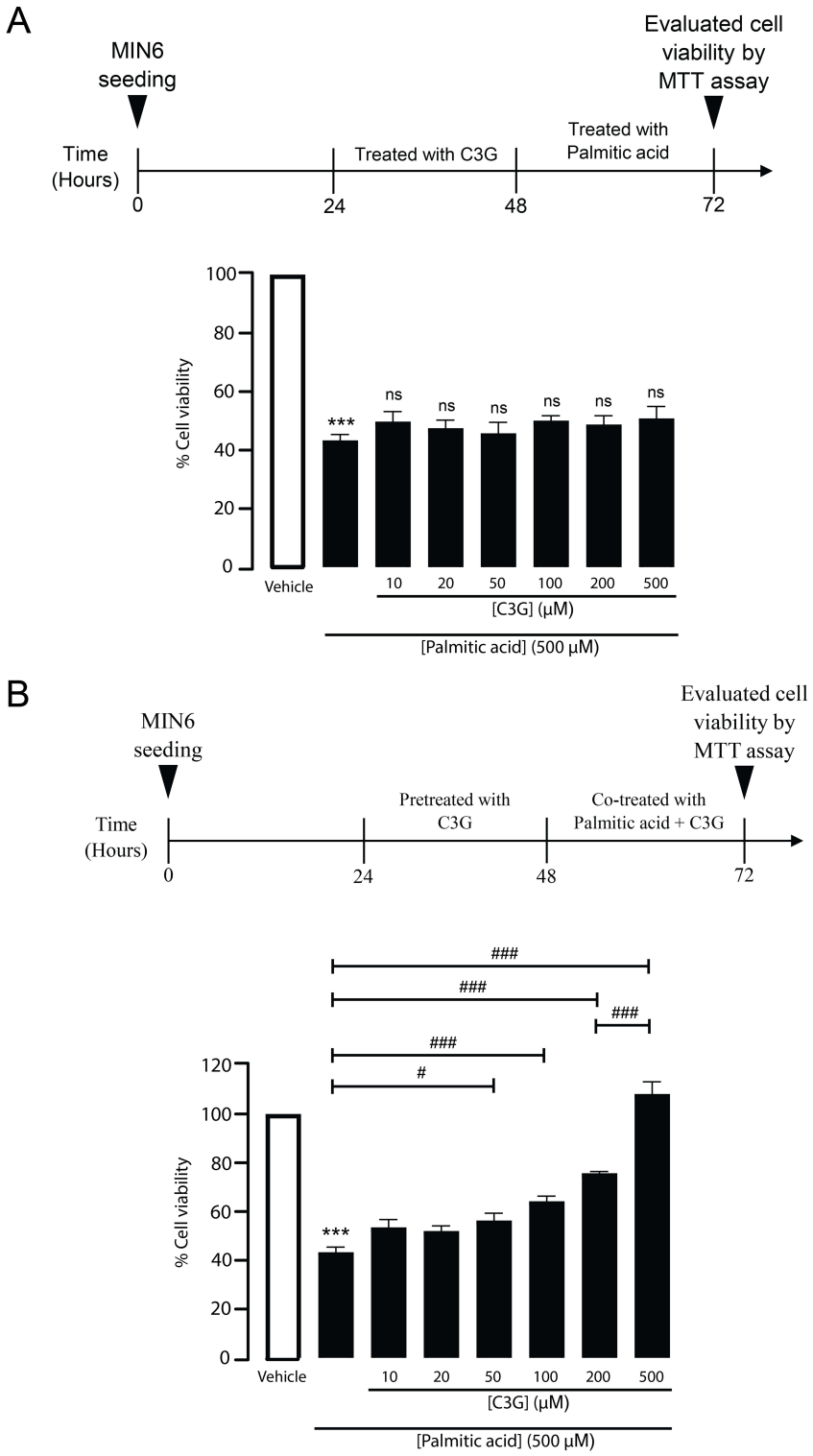

Figure 6 Assessment of the protective effect of Cyanidin 3-O-glucoside (C3G) pretreatment against palmitic acid (PA)-induced cytotoxicity in MIN6 cells. (**A**) Pretreatment effect of C3G at varying concentrations on MIN6 cell viability following PA exposure. Upper inset represents MIN6 cells initially treated with vary concentrations of C3G, followed by exposure to 500 μM PA. Cell viability was assessed by measuring absorbance at 573 nm. ***p < 0.001, PA-treated group compared to the vehicle group; ns, no significant difference between any C3G pretreated group and PA alone. Data are presented as mean ± S.E.M. (n = 4, representing four independent cell preparations; each condition measured in duplicate). (**B**) Co-treatment condition of C3G enhances MIN6 cell viability in a dose-dependent manner during PA exposure. Lower inset showed cells pretreated with vary concentration of C3G and subsequently co-treated with PA under the same C3G concentrations. Cell viability was quantified by measuring absorbance at 573 nm. ***p < 0.001, PA-treated group (500 μM) compared to the vehicle group; $^{\#}$p<0.05 compared to PA-treated group (for PA + C3G 50 μM); $^{\#\#\#}$p < 0.001 compared to PA-treated group (for PA + C3G at 100, 200, and 500 μM), and between PA + C3G 500 μM and PA + C3G 200 μM groups. Values are expressed as mean ± S.E.M (n = 4, representing four independent cell preparations; each condition measured in duplicate).

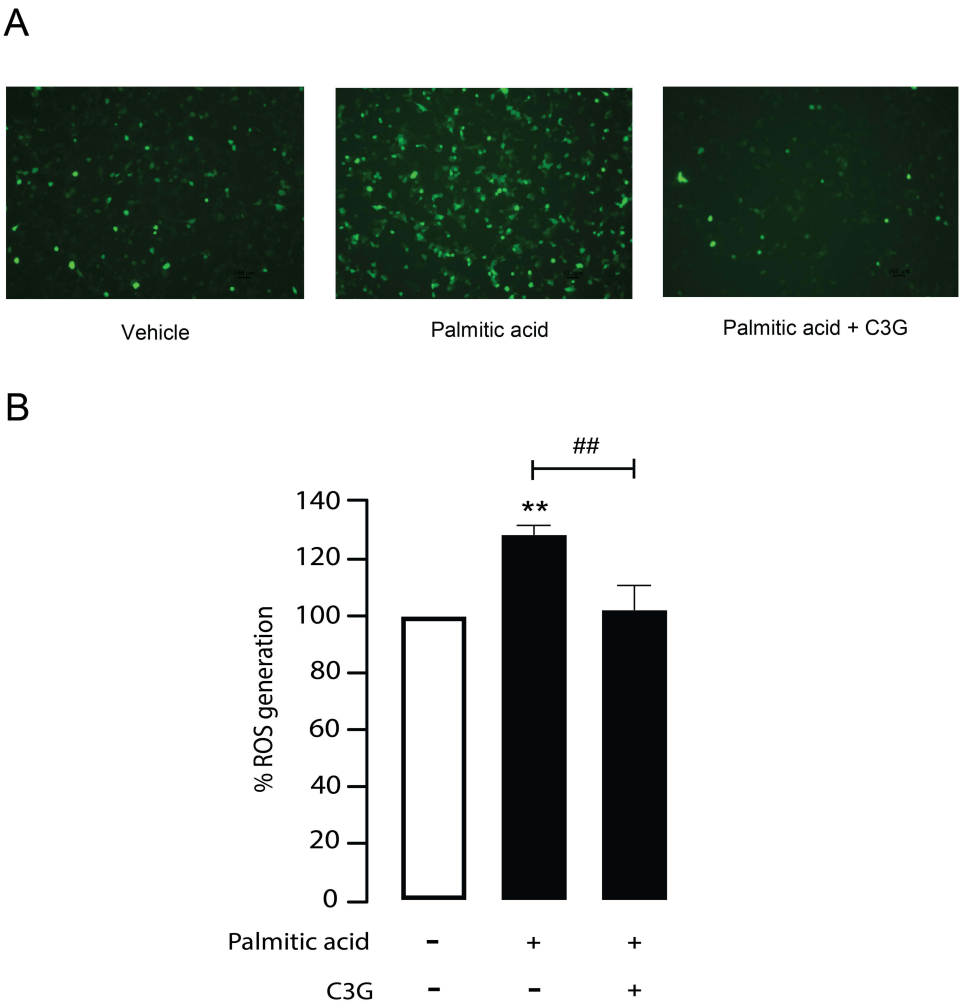

Figure 7 Antioxidant potential of Cyanidin 3-O-glucoside (C3G) against palmitic acid (PA)-mediated reactive oxygen species (ROS) generation. (**A**) Representative fluorescence images of intracellular ROS generation in MIN6 cells. Green fluorescence indicates ROS levels in vehicle, PA-treated, and PA plus C3G-treated groups. Imaging was performed with excitation and emission wavelengths of 485 nm and 535 nm, respectively. (**B**) Quantified fluorescence intensity is presented as a bar graph, representing ROS levels as a percentage of vehicle. **p < 0.01, PA-treated group compared to vehicle; ##p < 0.01, PA-treated group compared to PA + C3G 500 μM. Data are expressed as mean ± S.E.M (n = 5, representing five independent cell preparations; each condition measured in duplicate).

Evaluation of the Antioxidant Capacity of C3G via Its Radical Scavenging Activity

Given that C3G exhibits antioxidative properties, particularly when co-administered during lipotoxic stress, it is plausible that C3G may reduce intracellular ROS accumulation through direct radical scavenging. To test this hypothesis, a DPPH assay was conducted to assess the free radical scavenging activity of C3G, as illustrated in Figure 8A. The results showed that C3G exhibited dose-dependent DPPH radical scavenging activity, with increasing concentrations yielding higher activity compared to the positive control, Trolox (Figure 8B). Importantly, C3G demonstrated maximal free radical-scavenging activity at 500 μM, reaching approximately 90% (90 ± 3.8, ns, compared to the corresponding Trolox-treated group). These findings suggest that C3G attenuates ROS accumulation, at least in part, through direct radical neutralization.

Antioxidant Effect of High-Concentration C3G Protects β-Cells from PA-Induced Apoptosis via ER Stress Pathway

PA is known to induce β-cell apoptosis through excessive ROS accumulation and ER stress.[37] To investigate whether C3G could directly neutralize PA-induced ROS and thereby suppress ER stress-mediated apoptotic signaling, Western blot analysis was performed. MIN6 cells were treated with PA (500 μM) in the presence or absence of high-dose C3G

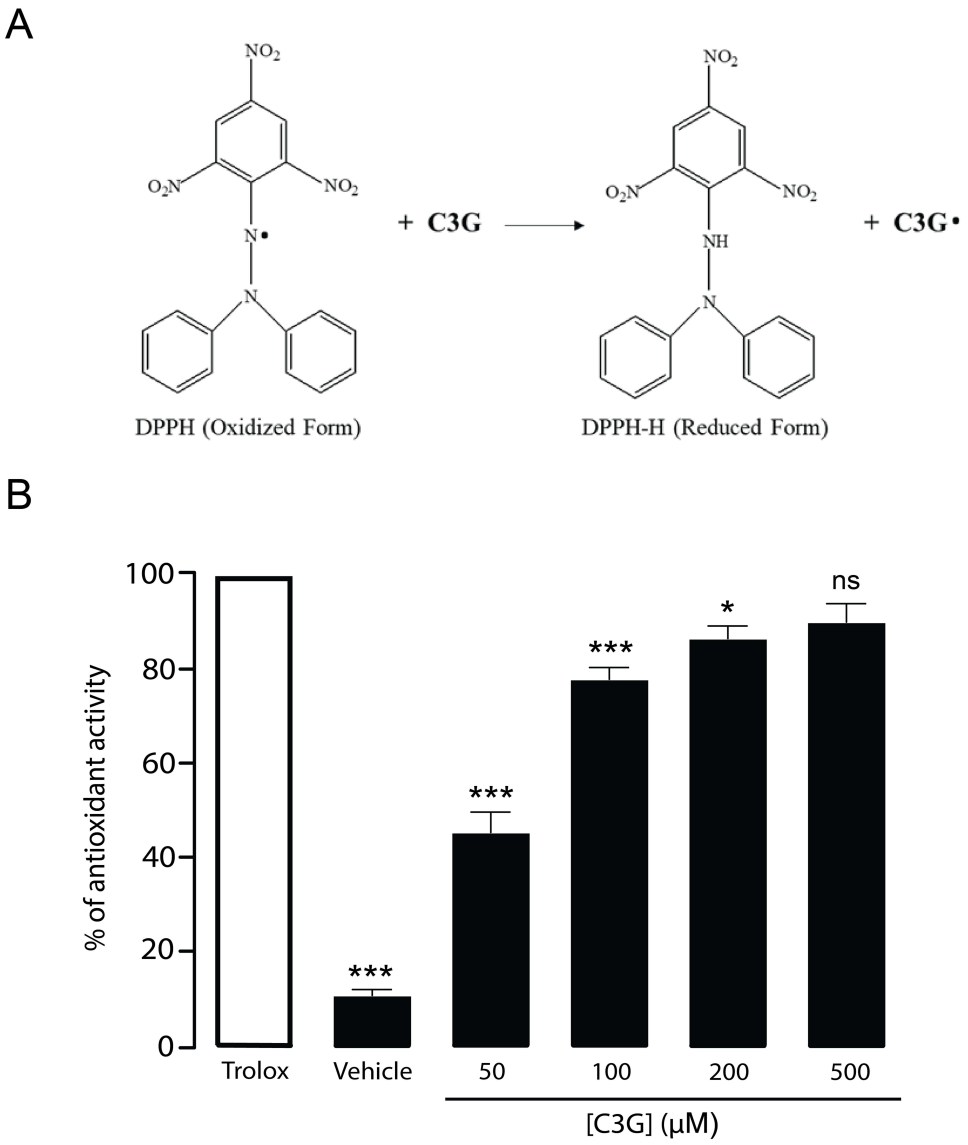

Figure 8 Antioxidant mechanism of Cyanidin 3-O-glucoside (C3G) in protecting against reactive oxygen species (ROS) generation. (**A**) Illustrated image shows the method used to assess the free radical scavenging activity of C3G via the DPPH assay. The reduction of the purple DPPH solution to yellow reflects antioxidant activity, which was quantified by measuring absorbance at 517 nm. (**B**) The antioxidant activity of C3G was evaluated in a dose-dependent manner at concentrations of 50, 100, 200, and 500 μM, and compared to Trolox at equivalent concentrations as a positive control. *p < 0.05; ***p < 0.001; ns, not statistically significant compared to the corresponding Trolox-treated group. The vehicle group, in the absence of C3G, represented the baseline data. Data are presented as mean ± S.E.M (n = 4, representing four independent cell preparations; each condition measured in duplicate).

(500 μM) for 24 hours. Protein extracts were collected to evaluate CHOP and cleaved caspase-3 expression as markers of ER stress and apoptosis, respectively. The results demonstrated that PA markedly increased CHOP and cleaved caspase-3 expression by 1.86-fold (186.3 ± 18.9; **p < 0.01 vs vehicle) and 1.81-fold (181.1 ± 25.5; **p < 0.01 vs vehicle), respectively. In contrast, co-treatment with C3G significantly downregulated both markers (CHOP: 105.6 ± 18.9; cleaved caspase-3: 106.6 ± 25.5; $^{\#\#}$p < 0.01 vs PA (500 μM) alone) (Figure 9A and B). These findings indicate that C3G exerts potent antioxidant activity by directly scavenging PA-induced ROS, thereby suppressing the downstream ER stress-dependent apoptotic pathway (Figure 10).

Discussion

T2DM is a chronic metabolic disorder characterized by low-grade inflammation, with obesity-related elevations in circulating free fatty acids, particularly PA, driving cytokine production, oxidative stress, and β-cell dysfunction.[38–41]

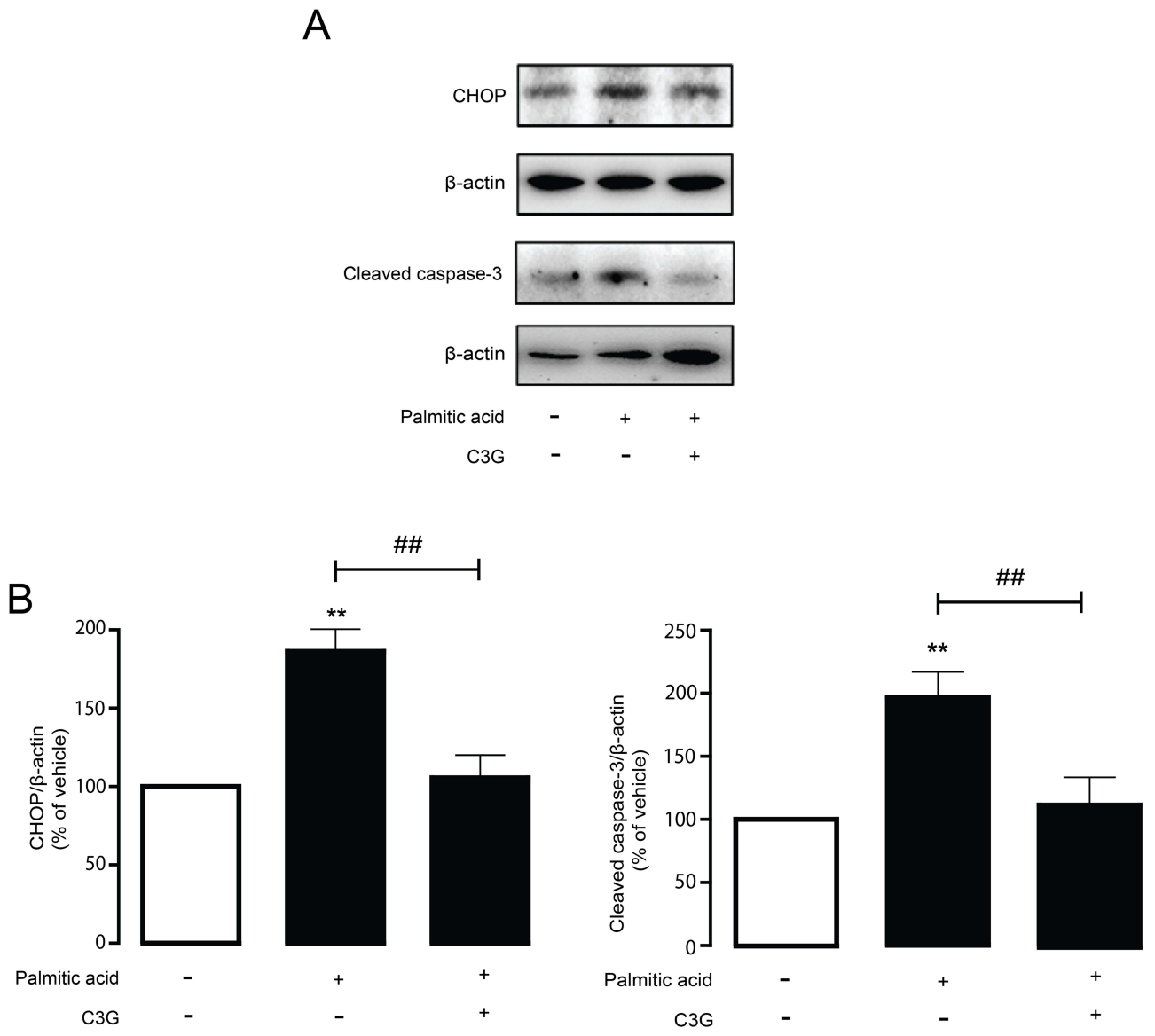

Figure 9 Effect of Cyanidin 3-O-glucoside (C3G) on palmitic acid (PA)-induced endoplasmic reticulum (ER) stress and apoptosis in MIN6 cells. Western blot analysis was performed to assess C/EBP homologous protein (CHOP) and cleaved caspase-3 expression as markers of ER stress and apoptotic signaling. MIN6 cells were treated with PA (500 μM) with or without C3G (500 μM) for 24 hours, and protein extracts were analyzed. (**A**) Representative immunoblots showing CHOP and cleaved caspase-3 expression across five independent experiments (n = 5). Bands illustrate vehicle, PA (500 μM)-treated, and PA plus C3G (500 μM)-treated groups. (**B**) Quantitative analysis of CHOP and cleaved caspase-3 expression normalized to β-actin. Data are presented as percentages relative to the vehicle group (mean ± S.E.M., n = 5 representing five independent cell preparations). Statistical analysis was performed using one-way ANOVA; $^{**}p < 0.01$ vs vehicle; $^{\#\#}p < 0.01$ vs PA (500 μM) alone.

Cyanidin-3-O-glucoside (C3G), a natural anthocyanidin with antioxidant activity, has been reported to protect β-cells, although its mechanisms under pre-oxidative conditions and at higher treatment levels remain undefined. Our study demonstrated that C3G dose-dependently protects MIN6 pancreatic β-cells from PA-induced cytotoxicity and apoptosis, with a prominent effect at high concentrations, observed only during co-exposure with PA. Mechanistic insights revealed that C3G reduces intracellular ROS through acute radical scavenging, highlighting its potential as a direct antioxidant therapeutic candidate against T2DM.

The MIN6 cell line, derived from murine insulinoma, is widely used to study pancreatic β-cell physiology and pathology because it retains glucose-stimulated insulin secretion and sustained insulin expression in early passages.[42,43] With high proliferative capacity and ease of culture, MIN6 provides a reliable model for investigating β-cell dysfunction induced by saturated fatty acids such as PA.[44,45] PA, a major circulating free fatty acid, is implicated in inflammation and

https://doi.org/10.2147/JEP.S562755

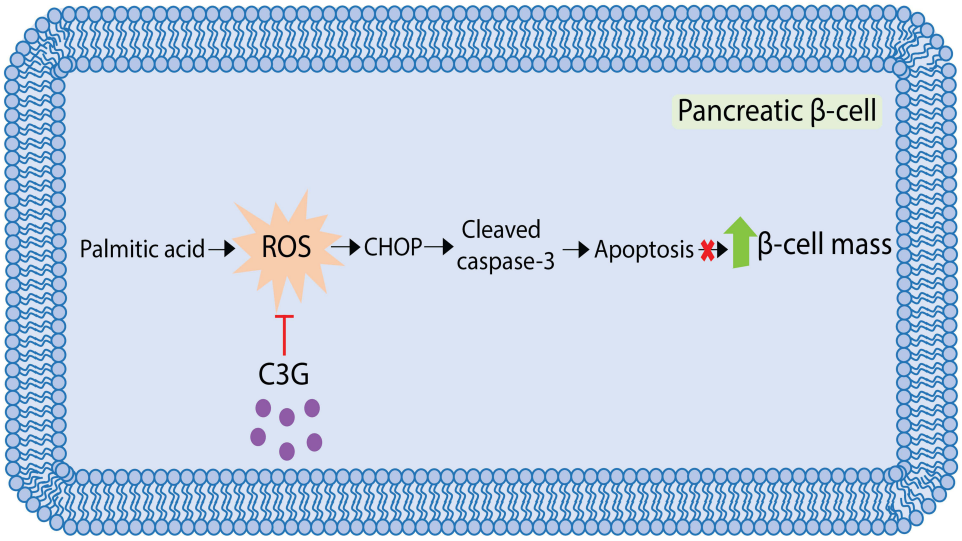

Figure 10 Schematic illustration of Cyanidin 3-O-glucoside (C3G) in protecting against intracellular reactive oxygen species (ROS)-induced apoptosis in MIN6 cells.

β-cell toxicity in T2DM.[39,46] In our study, PA exposure markedly reduced MIN6 viability by promoting apoptosis through intracellular ROS generation, consistent with previous reports that PA-induced oxidative stress drives β-cell death and T2DM progression.[38,41] This mechanism likely involves ROS accumulation, oxidative damage, and impaired ATP production,[47] while chronic PA exposure further downregulated antioxidant enzymes including catalase (CAT) and superoxide dismutase (SOD), thereby amplifying oxidative stress, apoptosis, and progressive β-cell failure.[23–25] Interestingly, in our experiments, PA at 50 μM decreased cell viability (Figure 2), suggesting heightened β-cell sensitivity to saturated fatty acids. This may reflect differences between human and in vitro conditions. In humans, circulating PA (~50–150 μM) is >99% bound to serum albumin, leaving only a nanomolar free fraction available to cells.[48] While albumin buffering prevents lipotoxicity in humans, serum-free culture exposes β-cells to disproportionately high levels of unbound PA. Thus, even physiological concentrations can induce cytotoxicity in vitro. Moreover, 500 μM PA produced the maximal reduction in β-cell viability, and increasing to 1000 μM did not cause further significant cell death. This plateau effect has been reported previously and is attributed to solubility limits of PA in culture medium and saturation of apoptotic pathways.[49]

Cyanidin-3-O-glucoside (C3G), a dietary anthocyanin, is recognized for its cytoprotective effects in pancreatic β-cells; however, the onset and mechanistic basis of its action remain unclear, particularly under intensified lipotoxic conditions. Previous studies in INS-1 cells reported that low concentrations of C3G (≤50 μM) improved viability and reduced apoptosis induced by hydrogen peroxide or PA, with protection rates of ~30–40%.[50] These effects appear linked to activation of endogenous antioxidant pathways, including Nrf2-mediated transcription of heme oxygenase-1 (HO-1), mitochondrial stabilization, and regulation of cytoplasmic redox balance, triggered when excessive ROS disrupt cellular homeostasis.[33,51] Consistent with these findings, our study confirmed that low-dose C3G improved MIN6 cell viability under PA exposure, but was insufficient to fully counteract apoptosis.

In contrast, the present study extends prior observations by systematically examining a substantially higher concentration of C3G (500 μM), which provided stronger protection (~80% recovery of viability) during concurrent PA exposure. This protective effect was observed specifically under continuous co-treatment conditions and was associated with significant reduction of intracellular ROS, consistent with a rapid antioxidant action. Moreover, our data refine the understanding of its dose- and time-dependent effects, suggesting that high-dose C3G may confer protection primarily during acute oxidative stress conditions. These temporal findings offer additional insight beyond prior studies that focused primarily on pre-treatment paradigms or pathway modulation at lower C3G concentrations. Although high-dose C3G could interfere with MTT assay readings, as anthocyanins are pigmented antioxidants, our control experiment with C3G alone (Figure 3B) showed only a minor artificial increase in signal. At 500 μM, C3G did not induce cytotoxicity,

suggesting minimal assay interference. In addition, the marked reduction of intracellular ROS observed in DCFDA assays (Figure 7B) and the ~80–100% cytoprotective effect confirmed by flow cytometry and cell death assay (Figures 4B and 5B) support that C3G provided genuine intracellular protection rather than a colorimetric artifact. Although we did not include a positive control for apoptosis (eg, staurosporine), such a reference could further validate the dynamic range of the Annexin V assay. Future studies incorporating a standard apoptotic inducer would strengthen assay standardization and enhance the robustness of the observed protective effects. Altogether, these results suggest that low-dose C3G primarily engages endogenous defense mechanisms under moderate stress, whereas high-dose C3G also functions as a potent antioxidant, offering immediate cytoprotection during intense lipotoxic challenge. The relative contributions of these pathways remain uncertain and require systematic evaluation across dose ranges, exposure timings, and different β-cell models.

Our findings indicate that the protective effect of high-dose C3G was only observed during continuous co-exposure with PA, suggesting that sustained presence of the compound is required for efficacy. While the feasibility of 500 μM C3G in vivo and potential off-target effects remain uncertain, our data showed that even at this high dose, C3G did not induce cytotoxicity (Figure 3B), supporting a relatively wide therapeutic window compared with other polyphenols that exhibit cytostatic effects at high concentrations.[52] The requirement for continuous presence is consistent with the highly reactive and acute nature of ROS, which can overwhelm endogenous defenses if not persistently neutralized.[53] The significant reduction of intracellular ROS observed in our DCFDA assays further indicates that C3G acted within cells rather than solely in the extracellular medium (Figure 7B), supporting a genuine biological mechanism. The loss of protection upon pre-treatment alone suggests that efficacy may be primarily attributable to acute antioxidant scavenging. Nevertheless, in addition to non-enzymatic antioxidant activity, it remains possible that high-dose C3G exerts its effects through modulation of endogenous antioxidant pathways or a combination of both. Because the present study did not directly evaluate endogenous antioxidant signaling (eg, Nrf2 activation, SOD or catalase expression), the relative contributions of direct ROS scavenging versus activation of intracellular antioxidant systems cannot be determined and warrant systematic investigation in future studies.

Translating this observation to an in vivo context raises the possibility that frequent dosing or sustained-release formulations may be necessary to maintain effective concentrations within pancreatic tissue. It remains uncertain whether high-dose C3G can reach pancreatic islets in sufficient amounts to prevent apoptosis under chronic lipotoxic conditions. Addressing this will require validation in primary human islets and in diabetic mouse models, where bioavailability, pharmacokinetics, and long-term efficacy can be systematically assessed. Such studies will be essential to determine whether C3G can preserve β-cell function and glucose homeostasis in more complex physiological settings, thereby bridging the gap between in vitro findings and therapeutic application.

Conclusion

In summary, this study provides novel evidence that high-level C3G acts as a potent intracellular free radical scavenger, effectively neutralizing excessive ROS accumulation and offering robust protection against PA-induced oxidative stress in β-cells. These findings highlight the therapeutic potential of C3G as a highly efficacious, low-toxicity antioxidant candidate for mitigating β-cell dysfunction in the context of T2DM.

Acknowledgment

Wanchalerm Yenjai and Phongthon Kanjanasirirat provided technical support at the Excellent Center for Drug Discovery (ECDD) for cell death assay.

Funding

This work was supported by National Research Council of Thailand, Faculty of Medicine Ramathibodi Hospital, Mahidol University (to CM), and the Mahidol Medical Scholars (MSP) Program (to SC).

Disclosure

The author(s) report no conflicts of interest in this work.

References

1. Hassan S, Gujral UP, Quarells RC, et al. Disparities in diabetes prevalence and management by race and ethnicity in the USA: defining a path forward. *Lancet Diabetes Endocrinol*. 2023;11(7):509–524. doi:10.1016/S2213-8587(23)00129-8
2. He KJ, Wang H, Xu J, Gong G, Liu X, Guan H. Global burden of type 2 diabetes mellitus from 1990 to 2021, with projections of prevalence to 2044: a systematic analysis across SDI levels for the global burden of disease study 2021. *Front Endocrinol*. 2024;15:1501690. doi:10.3389/fendo.2024.1501690
3. Strati M, Moustaki M, Psaltopoulou T, Vryonidou A, Paschou SA. Early onset type 2 diabetes mellitus: an update. *Endocrine*. 2024;85(3):965–978. doi:10.1007/s12020-024-03772-w
4. Kahn SE. The relative contributions of insulin resistance and beta-cell dysfunction to the pathophysiology of Type 2 diabetes. *Diabetologia*. 2003;46(1):3–19. doi:10.1007/s00125-002-1009-0
5. Esser N, Legrand-Poels S, Piette J, Scheen AJ, Paquot N. Inflammation as a link between obesity, metabolic syndrome and type 2 diabetes. *Diabet Res Clin Pract*. 2014;105(2):141–150. doi:10.1016/j.diabres.2014.04.006
6. Sobczak AIS, Blindauer CA, Stewart AJ. Changes in plasma free fatty acids associated with type-2 diabetes. *Nutrients*. 2019;11(9):2022.
7. Fatima S, Hu X, Gong RH, et al. Palmitic acid is an intracellular signaling molecule involved in disease development. *Cell Mol Life Sci*. 2019;76(13):2547–2557. doi:10.1007/s00018-019-03092-7
8. Gao Z, Hwang D, Bataille F, et al. Serine phosphorylation of insulin receptor substrate 1 by inhibitor kappa B kinase complex. *J Biol Chem*. 2002;277(50):48115–48121. doi:10.1074/jbc.M209459200
9. Malkowska P. Positive effects of physical activity on insulin signaling. *Curr Issues Mol Biol*. 2024;46(6):5467–5487. doi:10.3390/cimb46060327
10. Tanti JF, Ceppo F, Jager J, Berthou F. Implication of inflammatory signaling pathways in obesity-induced insulin resistance. *Front Endocrinol*. 2012;3:181.
11. Zolotnik IA, Figueroa TY, Yaspelkis BB. Insulin receptor and IRS-1 co-immunoprecipitation with SOCS-3, and IKKalpha/beta phosphorylation are increased in obese Zucker rat skeletal muscle. *Life Sci*. 2012;91(15–16):816–822. doi:10.1016/j.lfs.2012.08.038
12. He Z, Liu Q, Wang Y, et al. The role of endoplasmic reticulum stress in type 2 diabetes mellitus mechanisms and impact on islet function. *PeerJ*. 2025;13:e19192. doi:10.7717/peerj.19192
13. Lytrivi M, Tong Y, Virgilio E, Yi X, Cnop M. Diabetes mellitus and the key role of endoplasmic reticulum stress in pancreatic beta cells. *Nat Rev Endocrinol*. 2025;21:546–563. doi:10.1038/s41574-025-01129-5
14. Biden TJ, Boslem E, Chu KY, Sue N. Lipotoxic endoplasmic reticulum stress, beta cell failure, and type 2 diabetes mellitus. *Trends Endocrinol Metab*. 2014;25(8):389–398.
15. Cnop M, Igoillo-Esteve M, Cunha DA, Ladriere L, Eizirik DL. An update on lipotoxic endoplasmic reticulum stress in pancreatic beta-cells. *Biochem Soc Trans*. 2008;36(Pt 5):909–915. doi:10.1042/BST0360909
16. Oh YS, Bae GD, Baek DJ, Park EY, Jun HS. Fatty acid-induced lipotoxicity in pancreatic beta-cells during development of type 2 diabetes. *Front Endocrinol*. 2018;9:384. doi:10.3389/fendo.2018.00384
17. Tan J, Li Y, Hou DX, Wu S. The effects and mechanisms of cyanidin-3-glucoside and its phenolic metabolites in maintaining intestinal integrity. *Antioxidants*. 2019;8(10):479. doi:10.3390/antiox8100479
18. Tsuda T, Horio F, Uchida K, Aoki H, Osawa T. Dietary cyanidin 3-O-beta-D-glucoside-rich purple corn color prevents obesity and ameliorates hyperglycemia in mice. *J Nutr*. 2003;133(7):2125–2130. doi:10.1093/jn/133.7.2125
19. Kurimoto Y, Shibayama Y, Inoue S, et al. Black soybean seed coat extract ameliorates hyperglycemia and insulin sensitivity via the activation of AMP-activated protein kinase in diabetic mice. *J Agric Food Chem*. 2013;61(23):5558–5564. doi:10.1021/jf401190y
20. Oumeddour DZ, Al-Dalali S, Zhao L, Zhao L, Wang C. Recent advances on cyanidin-3-O-glucoside in preventing obesity-related metabolic disorders: a comprehensive review. *Biochem Biophys Res Commun*. 2024;729:150344. doi:10.1016/j.bbrc.2024.150344
21. Shi M, Mathai ML, Xu G, Su XQ, McAinch AJ. The effect of dietary supplementation with blueberry, cyanidin-3-O-beta-glucoside, yoghurt and its peptides on gene expression associated with glucose metabolism in skeletal muscle obtained from a high-fat-high-carbohydrate diet induced obesity model. *PLoS One*. 2022;17(9):e0270306. doi:10.1371/journal.pone.0270306
22. Yamashita Y, Wang L, Nanba F, Ito C, Toda T, Ashida H. Procyanidin promotes translocation of glucose transporter 4 in muscle of mice through activation of insulin and AMPK signaling pathways. *PLoS One*. 2016;11(9):e0161704. doi:10.1371/journal.pone.0161704
23. Rahman S, Mathew S, Nair P, Ramadan WS, Vazhappilly CG. Health benefits of cyanidin-3-glucoside as a potent modulator of Nrf2-mediated oxidative stress. *Inflammopharmacology*. 2021;29(4):907–923. doi:10.1007/s10787-021-00799-7
24. Ye X, Chen W, Tu P, et al. Food-derived cyanidin-3-O-glucoside alleviates oxidative stress: evidence from the islet cell line and diabetic db/db mice. *Food Funct*. 2021;12(22):11599–11610. doi:10.1039/D1FO02385C
25. Zhang B, Buya M, Qin W, et al. Anthocyanins from Chinese bayberry extract activate transcription factor Nrf2 in beta cells and negatively regulate oxidative stress-induced autophagy. *J Agric Food Chem*. 2013;61(37):8765–8772. doi:10.1021/jf4012399
26. Liu Y, Wang Q, Wu K, et al. Anthocyanins' effects on diabetes mellitus and islet transplantation. *Crit Rev Food Sci Nutr*. 2023;63(33):12102–12125. doi:10.1080/10408398.2022.2098464
27. Dodd S, Dean O, Copolov DL, Malhi GS, Berk M. N-acetylcysteine for antioxidant therapy: pharmacology and clinical utility. *Expert Opin Biol Ther*. 2008;8(12):1955–1962. doi:10.1517/14728220802517901
28. Giordano ME, Caricato R, Lionetto MG. Concentration dependence of the antioxidant and prooxidant activity of trolox in HeLa cells: involvement in the induction of apoptotic volume decrease. *Antioxidants*. 2020;9(11):1058. doi:10.3390/antiox9111058
29. Schuurman M, Wilson RB, Borradaile N, Wang R. The antioxidant, N-acetyl-L-cysteine, affects beta cell oxidative stress, insulin secretion, and intracellular signaling pathways in MIN6 cells. *Cell Tissue Res*. 2025;402(3):267–281. doi:10.1007/s00441-025-04020-x
30. Giordano ME, Lionetto MG. Intracellular dual behavior of trolox in HeLa cells and 3T3 fibroblasts under basal and H(2)O(2)-induced oxidative stress conditions. *Molecules*. 2025;30(18):3755. doi:10.3390/molecules30183755
31. Li D, Zhang Y, Liu Y, Sun R, Xia M. Purified anthocyanin supplementation reduces dyslipidemia, enhances antioxidant capacity, and prevents insulin resistance in diabetic patients. *J Nutr*. 2015;145(4):742–748. doi:10.3945/jn.114.205674
32. Kaewin S, Changsorn K, Sungkaworn T, et al. Fungus-derived 3-hydroxyterphenyllin and candidusin A ameliorate palmitic acid-induced human podocyte injury via anti-oxidative and anti-apoptotic mechanisms. *Molecules*. 2022;27(7):2109. doi:10.3390/molecules27072109

33. Hu S, Kuwabara R, de Haan BJ, Smink AM, de Vos P. Acetate and butyrate improve beta-cell metabolism and mitochondrial respiration under oxidative stress. *Int J Mol Sci*. 2020;21(4):1542. doi:10.3390/ijms21041542
34. Palomer X, Pizarro-Delgado J, Barroso E, Vazquez-Carrera M. Palmitic and oleic acid: the yin and yang of fatty acids in type 2 diabetes mellitus. *Trends Endocrinol Metab*. 2018;29(3):178–190. doi:10.1016/j.tem.2017.11.009
35. Nemecz M, Constantin A, Dumitrescu M, et al. The distinct effects of palmitic and oleic acid on pancreatic beta cell function: the elucidation of associated mechanisms and effector molecules. *Front Pharmacol*. 2018;9:1554. doi:10.3389/fphar.2018.01554
36. Sramek J, Nemcova-Furstova V, Kovar J. Molecular mechanisms of apoptosis induction and its regulation by fatty acids in pancreatic beta-cells. *Int J Mol Sci*. 2021;22(8):4285. doi:10.3390/ijms22084285
37. Liu X, Zeng X, Chen X, et al. Oleic acid protects insulin-secreting INS-1E cells against palmitic acid-induced lipotoxicity along with an amelioration of ER stress. *Endocrine*. 2019;64(3):512–524. doi:10.1007/s12020-019-01867-3
38. Chen B, Li T, Wu Y, et al. Lipotoxicity: a new perspective in type 2 diabetes mellitus. *Diabetes Metab Syndr Obes*. 2025;18:1223–1237. doi:10.2147/DMSO.S511436
39. Gonzalez LL, Garrie K, Turner MD. Type 2 diabetes - An autoinflammatory disease driven by metabolic stress. *Biochim Biophys Acta Mol Basis Dis*. 2018;1864(11):3805–3823. doi:10.1016/j.bbadis.2018.08.034
40. Hameed I, Masoodi SR, Mir SA, Nabi M, Ghazanfar K, Ganai BA. Type 2 diabetes mellitus: from a metabolic disorder to an inflammatory condition. *World J Diabetes*. 2015;6(4):598–612. doi:10.4239/wjd.v6.i4.598
41. Ly LD, Xu S, Choi SK, et al. Oxidative stress and calcium dysregulation by palmitate in type 2 diabetes. *Exp Mol Med*. 2017;49(2):e291. doi:10.1038/emm.2016.157
42. Ishihara H, Asano T, Tsukuda K, et al. Pancreatic beta cell line MIN6 exhibits characteristics of glucose metabolism and glucose-stimulated insulin secretion similar to those of normal islets. *Diabetologia*. 1993;36(11):1139–1145. doi:10.1007/BF00401058
43. Miyazaki J, Araki K, Yamato E, et al. Establishment of a pancreatic beta cell line that retains glucose-inducible insulin secretion: special reference to expression of glucose transporter isoforms. *Endocrinology*. 1990;127(1):126–132. doi:10.1210/endo-127-1-126
44. El-Assaad W, Buteau J, Peyot ML, et al. Saturated fatty acids synergize with elevated glucose to cause pancreatic beta-cell death. *Endocrinology*. 2003;144(9):4154–4163. doi:10.1210/en.2003-0410
45. Maedler K, Spinas GA, Lehmann R, et al. Glucose induces beta-cell apoptosis via upregulation of the Fas receptor in human islets. *Diabetes*. 2001;50(8):1683–1690. doi:10.2337/diabetes.50.8.1683
46. Rohm TV, Meier DT, Olefsky JM, Donath MY. Inflammation in obesity, diabetes, and related disorders. *Immunity*. 2022;55(1):31–55. doi:10.1016/j.immuni.2021.12.013
47. Chen S, Li Q, Shi H, Li F, Duan Y, Guo Q. New insights into the role of mitochondrial dynamics in oxidative stress-induced diseases. *Biomed Pharmacother*. 2024;178:117084.
48. Huber AH, Kleinfeld AM. Unbound free fatty acid profiles in human plasma and the unexpected absence of unbound palmitoleate. *J Lipid Res*. 2017;58(3):578–585. doi:10.1194/jlr.M074260
49. Lytrivi M, Castell AL, Poitout V, Cnop M. Recent insights into mechanisms of beta-cell lipo- and glucolipotoxicity in type 2 diabetes. *J Mol Biol*. 2020;432(5):1514–1534. doi:10.1016/j.jmb.2019.09.016
50. Chen Y, Li X, Su L, et al. Cyanidin-3-O-glucoside ameliorates palmitic-acid-induced pancreatic beta cell dysfunction by modulating CHOP-mediated endoplasmic reticulum stress pathways. *Nutrients*. 2022;14(9):1835. doi:10.3390/nu14091835
51. Choi KH, Park MH, Lee HA, Han JS. Cyanidin-3-rutinoside protects INS-1 pancreatic beta cells against high glucose-induced glucotoxicity by apoptosis. *Z Naturforsch C J Biosci*. 2018;73(7–8):281–289. doi:10.1515/znc-2017-0172
52. Fulda S. Resveratrol and derivatives for the prevention and treatment of cancer. *Drug Discov Today*. 2010;15(17–18):757–765. doi:10.1016/j.drudis.2010.07.005
53. Beckhauser TF, Francis-Oliveira J, De Pasquale R. Reactive oxygen species: physiological and physiopathological effects on synaptic plasticity. *J Exp Neurosci*. 2016;10(Suppl 1):23–48. doi:10.4137/JEN.S39887